

Analyzing Time-dependent Neutrino Accretion Disc in Gamma-Ray Bursts

Michał Przerwa^{1,2} and Agnieszka Janiuk¹

1. Center for Theoretical Physics, Polish Academy of Sciences, Al. Lotników 32/46, 02-668 Warsaw, Poland

2. Physics Dept., University of Warsaw, Pasteura 5, 02-093 Warsaw, Poland

We analyze the conditions in a black hole's accretion disc under β -equilibrium and neutrino cooling. Such conditions are adequate for the central engine that powers relativistic jets in Gamma Ray Bursts. The disk wind will also produce species under r-process nucleosynthesis.

1 Model

Our analysis is based on the one used in Janiuk et al. (2007). We simulate the conditions in an accretion disc using different initial values of accretion rate (\dot{M}), the viscosity coefficient (α) and changing the black hole angular momentum ($a = cJ/GM^2$). For the disc viscous stress we use α viscosity prescription: $\tau_{r\varphi} = -\alpha P$ where P is the total pressure. Equations that describe the effect of black hole rotation on the structure of the accretion disk, involve the general relativistic corrections and have been presented in Janiuk & Yuan (2010). We adopt the mass of a black hole to be $3 M_\odot$. We integrate the disk structure equations and obtain its initial state ($t=0$), and then we evolve it to see a changing distribution of the amount of mass with a given electron fraction $M(Y_e)$, defined as:

$$Y_e = \frac{n_{e^-} - n_{e^+}}{n_b}, \quad (1)$$

where n_x is number density of x particle, and n_b is baryon number density. The range of Y_e in the disk is from 0.1 to 0.5, but can be as low as 0.015, for large accretion rates, hence such disks are strongly neutronized (see Fig. 1).

2 Results

We set the values of α and a to 0.1 and 0, respectively, and ran the simulation for accretion rates of 1, 10 and $12 M_\odot s^{-1}$. We then visualize the results on a plot of total pressure (P_{tot}), mass fraction of free nucleons (X_{nuc}) and electron fraction (Y_e) as a function of radius (Fig.1). On that plot we can see, that increasing the accretion rate, leads to increase in total pressure in the disc. Also, the mass fraction of free nucleons becomes small for large accretion rates in the outskirts of accretion disk, which is due to formation of Helium nuclei.

We run simulation with several different combinations of parameters, namely accretion rate, viscosity parameter and black hole spin. We plot the distribution of temperature, density, viscous heating, as well as electron fraction, neutrino cooling, and advective cooling as a function of radius (Fig.2).

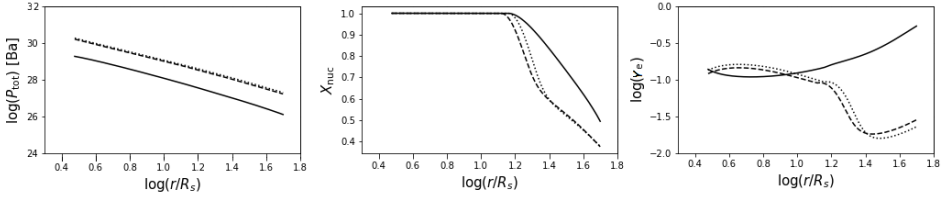


Fig. 1: Total pressure in the disc, mass fraction of free nucleons and electron fraction as a function of radius, plotted for accretion rates of $1 \text{ M}_\odot \text{s}^{-1}$ (solid line), $10 \text{ M}_\odot \text{s}^{-1}$ (dashed line) and $12 \text{ M}_\odot \text{s}^{-1}$ (dotted line).

The results are similar if the simulations are varying only in accretion rate, implying that the main differences are caused by the different viscosity and black hole spin coefficients.

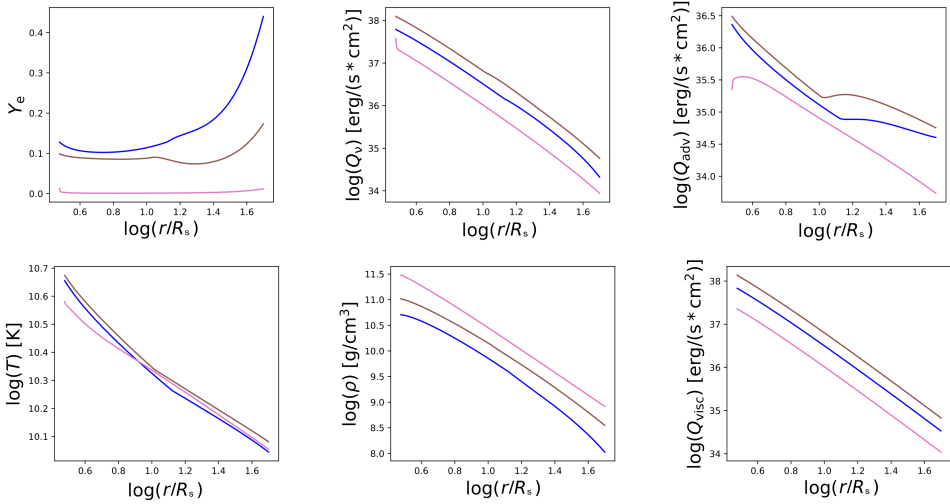


Fig. 2: Distribution of the temperature, density, viscous heating, electron fraction, neutrino cooling and advective cooling as a function of radius for different parameters. The parameters for the blue model are: $\dot{M} = 1 \text{ M}_\odot \text{s}^{-1}$, $\alpha = 0.1$, $a = 0.1$, for the brown: $\dot{M} = 2 \text{ M}_\odot \text{s}^{-1}$, $\alpha = 0.1$ and $a = 0.1$ and for the pink: $\dot{M} = 0.1 \text{ M}_\odot \text{s}^{-1}$, $\alpha = 0.01$ and $a = 0.6$

In order to see how the accretion disk evolves with time, and how its composition changes, we have plotted the histograms of the mass-binned electron fraction. The Y_e bins are distributed with width of 0.05 each. We repeated this procedure for several time snapshots. As the disk becomes advective, these distributions likely represent the typical values of the electron fraction in the viscously driven outflows that dominate subsequent mass loss (see Metzger et al. (2009)), as shown in the Figures 3-6.

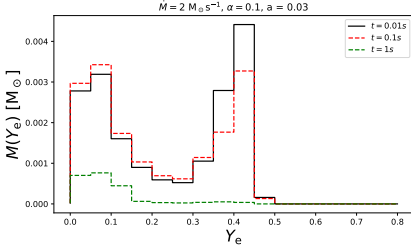


Fig. 3: Amount of mass in given range of electron fraction in three snapshots, at $t = 0.01s$, $t = 0.1s$ and $t = 1s$. Model parameters: $\dot{M} = 2 M_{\odot} s^{-1}$, $\alpha = 0.1$ and $a = 0.03$.

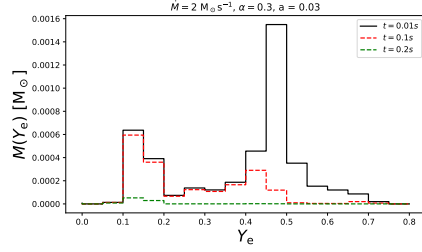


Fig. 4: Amount of mass in given range of electron fraction in three snapshots, at $t = 0.01s$, $t = 0.1s$ and $t = 0.2s$. Model parameters: $\dot{M} = 2 M_{\odot} s^{-1}$, $\alpha = 0.3$ and $a = 0.03$.

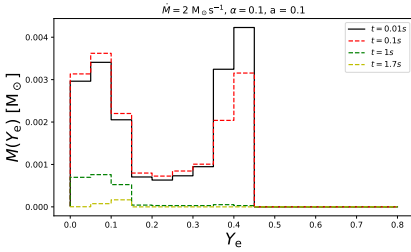


Fig. 5: Amount of mass in given range of electron fraction in three snapshots, at $t = 0.01s$, $t = 0.1s$, $t = 1s$ and $t = 1.7s$. Model parameters: $\dot{M} = 2 M_{\odot} s^{-1}$, $\alpha = 0.1$ and $a = 0.1$.

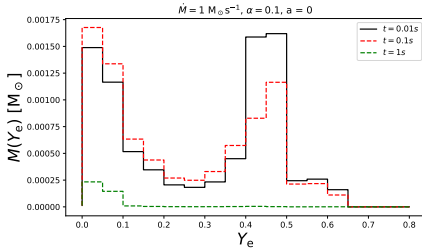


Fig. 6: Amount of mass in given range of electron fraction in three snapshots, at $t = 0.01s$, $t = 0.1s$ and $t = 1s$. Model parameters: $\dot{M} = 1 M_{\odot} s^{-1}$, $\alpha = 0.1$ and $a = 0$.

3 Conclusions

We find that the initial distribution of electron fraction in our disk is bi-modal, with large mass contribution of both highly neutronized material $Y_e < 0.1$, and weakly neutronized, $Y_e \sim 0.5$. This distribution is found for large accretion rate ($\dot{M} = 2 M_{\odot} s^{-1}$) and large viscosity ($\alpha = 0.1, 0.3$) models. As the time evolution proceeds, the total mass of the disk decreases, but the contribution of neutron rich material, is still larger than the neutron poor fraction. For smaller accretion rate ($\dot{M} = 1 M_{\odot} s^{-1}$), and/or smaller viscosity, ($\alpha = 0.03$), the distribution of electron fraction favours most mass is contained in neutron-rich material. This result is consistent with findings of Metzger et al. (2009), who also studied models with small accretion rates.

Acknowledgements. This research was supported in part by the Polish National Science Center grant No. DEC-2019/35/B/ST9/04000.

References

- Janiuk, A., Yuan, Y., *A&A* **509**, 9 pp. (2010)
- Janiuk, A., Yuan, Y., Perna, R., Di Matteo, T., *ApJ* **664**, 2, 1011 (2007)
- Metzger, B. D., Piro, A. L., Quataert, E., *MNRAS* **396**, 1, 304 (2009)